Sensors & Actuators: B. Chemical 353 (2022) 131000

Contents lists available at ScienceDirect

Sensors and Actuators: B. Chemical

journal homepage: www.elsevier.com/locate/snb

A distyrylbenzene-based fluorescent probe with high photostability and large Stokes shift for STED nanoscopy imaging of cellular lipid droplets

Guannan Liu [a], Jianan Dai [a], Ri Zhou [a], Guishan Peng [a], Chenguang Wang [a,*], Xu Yan [a], Xiaoteng Jia [a], Xiaomin Liu [a], Yuan Gao [a], Lijun Wang [a,b], Geyu Lu [a,*]

[a] State Key Laboratory of Integrated Optoelectronics, Key Laboratory of Advanced Gas Sensors of Jilin Province, College of Electronic Science and Engineering, Jilin University, Changchun 130012, People's Republic of China

[b] State Key Laboratory of Luminescence and Applications, Changchun Institute of Optics, Fine Mechanics and Physics, Chinese Academy of Sciences, Changchun 130033, People's Republic of China

ARTICLE INFO

Keywords:
Fluorescence imaging
Nanoscopy imaging
STED imaging
Organic fluorescent probes
Lipid droplets

ABSTRACT

Directly limited by the availability of suitable organic fluorescent probes, the stimulated emission depletion (STED) nanoscopy imaging of cellular lipid droplets (LDs) is a highly challenge task. Herein, a sulfone-embedded distyrylbenzene derivative SO2-DSB has been reported as a novel LDs fluorescent probe suitable for STED nanoscopy imaging. This fluorescent probe exhibiting high photostability and large Stokes shift could be efficiently depleted while be not excited by the extremely strong STED lasers of 592 nm or 660 nm. Consequently, STED nanoscopy imaging of LDs employed with this fluorescent probe has achieved high resolutions of 73 nm and 84 nm under 592 nm and 660 nm STED lasers, respectively. Notably, these resolutions are significantly higher than the common confocal images (resolutions of about 250 nm) and represent one of the leading results of the nanoscopy imaging of LDs so far, highlight the ability of this fluorescent probe in STED nanoscopy. In addition, the general ability of this fluorescent probe in confocal microscopy has also been demonstrated by 3D imaging and multicolor imaging.

1. Introduction

Lipid droplets (LDs) are essential organelles existing in almost all eukaryotic cells. LDs are a kind of core-shell shaped spherical organelle of which the neutral lipids core is surrounded by the phospholipid monolayer membrane. In a long period, LDs were generally regarded as a kind of inert organelle that just stores fat lipids. However, the recent studies have continuously revealed the critical roles of LDs in a lot of cellular dynamic processes, such as the membrane trafficking, protein degradation, signal transduction and so on. Therefore, it has been regarded as one of the most appealing topics of cell biology to study new functions of LDs in the last decade [1–4].

Dependent on the types of cells, LDs are wildly changed in diameters [1,2]. For example, the diameters of LDs are around 10–200 μm in adipocytes, while only 100 nm–1 μm in brown adipose tissue. Additionally, the diameters of nascent LDs that are newly generated by releasing from endoplasmic reticulum (ER) are even less than 100 nm. The fluorescence imaging techniques (such as confocal and two-photon) have been widely employed to visualize LDs and investigate the multiple capabilities. Consequently, a lot of superior fluorescent probes have been successfully developed for the confocal or two-photon imaging of LDs [5–13]. However, the resolutions of these common fluorescence imaging techniques are intrinsically limited to be around 250 nm (half value of excitation wavelength) due to the light diffraction. Thus, these imaging techniques are not capable for visualizing the small nascent LDs, which largely limit the study of LDs in depth.

In this context, the nanoscopy fluorescence imaging techniques, which successfully break the light diffraction limit and provide a dramatically higher resolution than 250 nm, have attracted much attention very recently [14–16]. Among various nanoscopy imaging techniques, stimulated emission depletion (STED) nanoscopy is the most prevalent one, because it in principle could provide the highest spatial and temporal resolution. For STED nanoscopy imaging, it intrinsically requires that the fluorescent probe should display excellent photostability under the extremely strong STED laser as well as can be efficiently depleted but not be excited by the STED laser (*vide infra*) [17,18]. Because the existed organic fluorescent probes suitable for the confocal or two-photon imaging techniques generally do not fill these strict

* Corresponding authors.
E-mail addresses: wangchenguang@jlu.edu.cn (C. Wang), lugy@jlu.edu.cn (G. Lu).

https://doi.org/10.1016/j.snb.2021.131000
Received 18 August 2021; Received in revised form 13 October 2021; Accepted 24 October 2021
Available online 29 October 2021

requirements, the design and synthesis of superior fluorescent probes capable for STED nanoscopy imaging has attracted great interest. Accordingly, a few of new organic fluorescent probes with the specificity towards cellular organelles LDs [19–23], mitochondria [24,25], lysosomes [26], and so on [27–32], have been successfully developed recently for STED nanoscopy imaging. These reports not only highlight the advantage of high resolution of STED nanoscopy imaging over the common confocal/two-photon imaging, but also largely promote the relative study of cell biology on the nanoscale. However, the organic fluorescent probes which are capable for STED nanoscopy imaging are still very limited. Moreover, the performances of fluorescent probes in STED imaging, in terms of the resolution and the depletion efficiency, are required to be dramatically improved.

Herein, we developed a sulfone-embedded distyrylbenzene derivative SO2-DSB (Fig. 1a) as a novel LDs fluorescent probe capable for STED nanoscopy imaging. This fluorescent probe exhibits high fluorescence brightness, good staining specificity toward LDs and high photostability. Importantly, the large Stokes shift of this probe enables to be easily depleted while be not excited by two commonly used STED lasers of 592 nm and 660 nm. Applying the fluorescent probe for STED nanoscopy imaging of LDs has obtained high resolutions of 73 nm and 84 nm under 592 nm and 660 nm STED lasers, respectively. These resolutions are significantly higher than the corresponding confocal images (resolutions of about 250 nm) and represent one of the leading results among the nanoscopy imaging of LDs up to date. Consequently, the small nearby LDs which cannot be separated in the confocal images have been successfully visualized one by one in the STED nanoscopy images. Besides of STED imaging, the superior utility of this fluorescent probe has been also demonstrated in the 3D confocal imaging as well as the four-color confocal imaging.

2. Results and discussion

2.1. Molecular design and synthesis of SO2-DSB

The molecular design of SO2-DSB is based on the 1,4-distyrylbenzene skeleton which is a classical fluorophore displaying intense emission (Fig. 1a). To significantly improve the photostability, two strong electron-withdrawing sulfone moieties are embedded into the distyrylbenzene skeleton. This strategy not only decreases the HOMO/LUMO energy levels of molecule [33,34], but also fixes the C=C double band avoiding the *cis-trans* isomerization of stilbene [35,36] (Supplementary Scheme S1). Moreover, two alkyl chains are introduced to the π-conjugated skeleton with the arm of tuning the hydrophobicity of fluorescent probe and thus resulting good staining specificity toward cellular LDs. The synthesis of fluorescent probe SO2-DSB is straightforward (Supplementary Scheme S2). Starting from the commercially available benzo[1,2-*b*:4,5-*b*′]dithiophene-4,8-dione, the key intermediate 2,6-dibromo-4,8-dipropoxybenzo[1,2-*b*:4,5-*b*′]dithiophene was readily obtained in three steps of reduction, alkalization and bromination. The dibromo intermediate was further proceeded Suzuki-Miyaura coupling reaction followed by oxidization of the S atoms, thus providing the target fluorescent probe SO2-DSB. The details of chemical synthesis and characterization data are shown in Supplementary material.

2.2. Photophysical property of SO2-DSB

The photophysical property of fluorescent probe SO2-DSB was studied in various organic solvents. The absorption (λ_{abs}) and emission (λ_{em}) maxima of probe are around 440 nm and 515 nm, respectively, which are insensitive to the solvent polarity (Fig. 1b and Table 1). Importantly, featuring with large Stokes shifts of about 75 nm, the probe displays good to high fluorescence quantum yields (Φ_F): 99% in nonpolar toluene, while still maintains 66% in high polar CH_3CN. The moderate separation between HOMO and LUMO causes the large Stokes shift (Supplementary Fig. S1). The fluorescence lifetimes (τ) of probe were also measured in various solvents (Supplementary Fig. S2–S5) and the radiative/non-radiative decay constants (k_r/k_{nr}) were thus calculated based on the values of τ and Φ_F (Table 1). In comparison to the other solvents ($k_{nr} < 0.2 \times 10^8\ s^{-1}$), the k_{nr} in CH_3CN ($1.2 \times 10^8\ s^{-1}$) is dramatically increased. Further theoretical calculation maybe helps to clarify the non-radiative decay process in CH_3CN. The fluorescence brightness of probe, which is defined as the multiplication value of the molar absorption coefficient (ε) and the Φ_F, is calculated to be $2.6 \times 10^4\ M^{-1}\ cm^{-1}$ in toluene. This fluorescence brightness is fine and even higher than Nile Red ($\sim 2.4 \times 10^4\ M^{-1}\ cm^{-1}$) which is a well-known and typical LDs fluorescent probe [5]. In comparison to the representative green-emissive probes (*e.g.* Abberior STAR GREEN, ATTO 488, Alexa Fluor 488) used in STED nanoscopy imaging, this probe SO2-DSB displays the feature of significantly large Stokes shift (Supplementary Table S1). Even in comparison to the probes Abberior STAR 440SX and Abberior STAR 520SXP which are specially developed as the large Stokes shift ones for STED imaging, the probe SO2-DSB is still a strong competitor in terms of the large Stokes shift as well as the high fluorescence brightness.

Notably, the large Stokes shift of fluorescent probe SO2-DSB enables to be capable for two commonly used STED lasers of 592 nm and 660 nm in STED nanoscopy imaging (Fig. 1b). Both STED lasers are away from the absorption edges (> 50 nm) to strictly avoid the re-excitation by STED lasers, while have significant overlap with the emission spectrum to facilitate the depletion process and thus to improve the resolution of

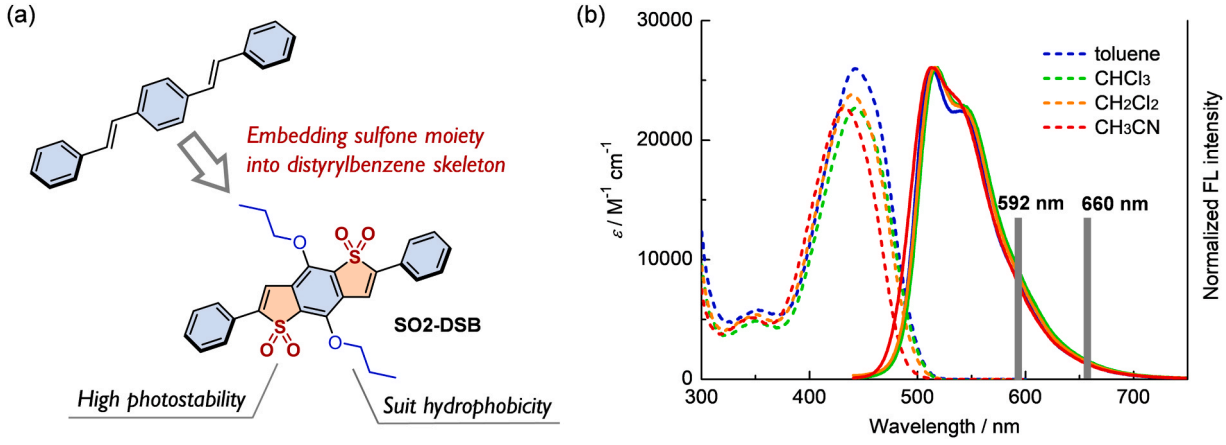

Fig. 1. (a) The molecular design of lipid droplets fluorescent probe SO2-DSB based on the distyrylbenzene skeleton. (b) Absorption and emission spectra of probe SO2-DSB (concentration of 1.00×10^{-5} M) in various solvents.

Table 1
Photophysical data for fluorescent probe SO2-DSB in various solvents.

Solvent	Δf[a]	λ_{abs} (nm)	ε (M^{-1} cm^{-1})	λ_{em} (nm)	Stokes shift (nm)	Φ_F[b]	τ (ns)	k_r (10^8 s^{-1})	k_{nr} (10^8 s^{-1})
Toluene	0.013	442	26,000	513	71	99%	3.55	2.8	0.03
$CHCl_3$	0.148	442	22,700	519	77	~ 100%	3.82	2.6	—
CH_2Cl_2	0.217	440	23,800	516	76	94%	3.69	2.5	0.16
CH_3CN	0.305	432	22,700	513	81	66%	2.77	2.4	1.2

[a] The solvent orientation polarizability.
[b] Absolute fluorescence quantum yield determined by a calibrated integrating sphere system.

imaging (*vide infra*). The fluorescent probe capable for two STED lasers means that much more choices of imaging conditions could be selected. This is a highly attractive advantage for the application of fluorescent probe in STED nanoscopy imaging.

2.3. LDs staining and confocal imaging of SO2-DSB

The cytotoxicity of fluorescent probe SO2-DSB was evaluated by the 3-(4,5-dimethylthia-zol-2-yl)-2,5-diphenyltetrazolium bromide (MTT) assay (Supplementary Fig. S6). The viability of Hela cells was not affected after incubation with 10 μM probe for 24 h. For the following biological imaging experiments, staining cells with a concentration of 2 μM probe (2 h) could provide enough fluorescence signal. The co-staining experiment of HeLa cells was conducted to reveal the cellular staining selectivity of the fluorescent probe SO2-DSB. Considering the absorption and emission spectra, this probe was paired with a highly specific LDs fluorescent probe Ph-Red [13]. Indeed, the fluorescence imaging channels of SO2-DSB and Ph-Red did not cross talk with each other (Supplementary Fig. S7). As shown in Fig. 2a, the imaging channel of SO2-DSB is finely overlapped with that of Ph-Red. The high value of Pearson's correlation coefficient ($R = 0.92$) strongly demonstrates the good staining selectivity of probe SO2-DSB towards cellular LDs (Supplementary Fig. S8). The LDs specificity of probe SO2-DSB was further proved by the multicolor confocal imaging. As shown in Fig. 2b and Supplementary Fig. S9, the imaging channels of LysoTracker Red and MitoTracker Deep Red do not overlap with that of SO2-DSB, directly excluding the possibility of staining lysosome and mitochondria by SO2-DSB. This experiment also highlights the utility of SO2-DSB as a LDs-specific fluorescent probe in multicolor confocal imaging that is a powerful tool to visualize different subcellular structures on the same images [6].

Importantly, the fluorescent probe SO2-DSB displays high photostability. The common used 488 nm laser was employed for the comparison of photostability between probes SO2-DSB and Nile Red, because this laser could excite both probes efficiently (Supplementary Fig. S10). Under the intense and identical excitation condition (λ_{exc} = 488 nm), the confocal images of HeLa cells stained with Nile Red or SO2-DSB were continuously recorded in the same area. As shown in Fig. 3a–b, the fluorescence signal of Nile Red is photobleached very quickly, while the signal of SO2-DSB is much more robust. After recording 50 confocal images, SO2-DSB still maintains 87% fluorescence signal of its initial value, which is largely higher than Nile Red (25%). The high photostability of SO2-DSB should be closely related to the molecular design of embedding strong electron-withdrawing sulfone moieties into the distyrylbenzene skeleton as before mentioned.

The high photostability of fluorescent probe SO2-DSB enables to conduct 3D confocal imaging, which is very useful to display the spatial distribution of biological interesting species [5,6]. In order to construct the 3D image, the sample is required to be imaged repeatedly to get a lot of Z-stack scanning slices. Therefore, the 3D imaging usually encounters the photobleaching problem of fluorescent probe. While the probe SO2-DSB displaying high photostability, it was readily applied in 3D imaging. The fixed HeLa cells were used in the 3D imaging experiment, because the LDs were highly dynamic species in living cells and the fast movement during the acquisition of Z-stack slices would decrease the quality of imaging result. To further improve the 3D image quality, the Z-stack slices were recorded under a small Z-step of 200 nm and a line average of two times per slice. Based on the 59 Z-stack slices (totally 118 imaging scans), the high-quality 3D confocal image with a Z-depth of 11.6 μm was successfully reconstructed (Fig. 4 and Supplementary Movie S1). Thus, the spatial distribution of LDs can be clearly visualized, highlighting the photostability and utility of SO2-DSB.

Supplementary material related to this article can be found online at doi:10.1016/j.snb.2021.131000.

2.4. STED nanoscopy imaging of SO2-DSB

STED nanoscopy imaging employs two lasers: one excitation laser similar to confocal imaging and one special donut-shape depletion laser (STED laser). The STED laser is extremely strong (about 10^2–10^3 M W cm^{-2}) to be able to quench the surrounding fluorescence of excitation spot *via* the stimulated emission depletion process and thus to

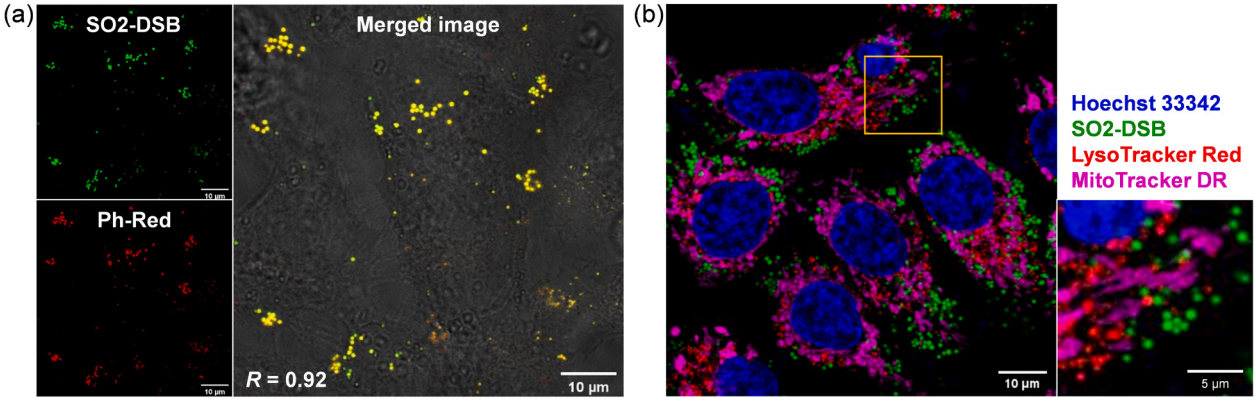

Fig. 2. (a) Confocal images of HeLa cells labeled with SO2-DSB and Ph-Red: the images of each fluorescence channels, the merged image of two fluorescence channels and bright field channel; scale bar: 10 μm. (b) Multicolor confocal image of HeLa cells labeled with Hoechst 33342, SO2-DSB, LysoTracker Red and MitoTracker Deep Red, respectively; scale bar: 10 μm. The inset shows zoomed view of the square marked region; scale bar: 5 μm.

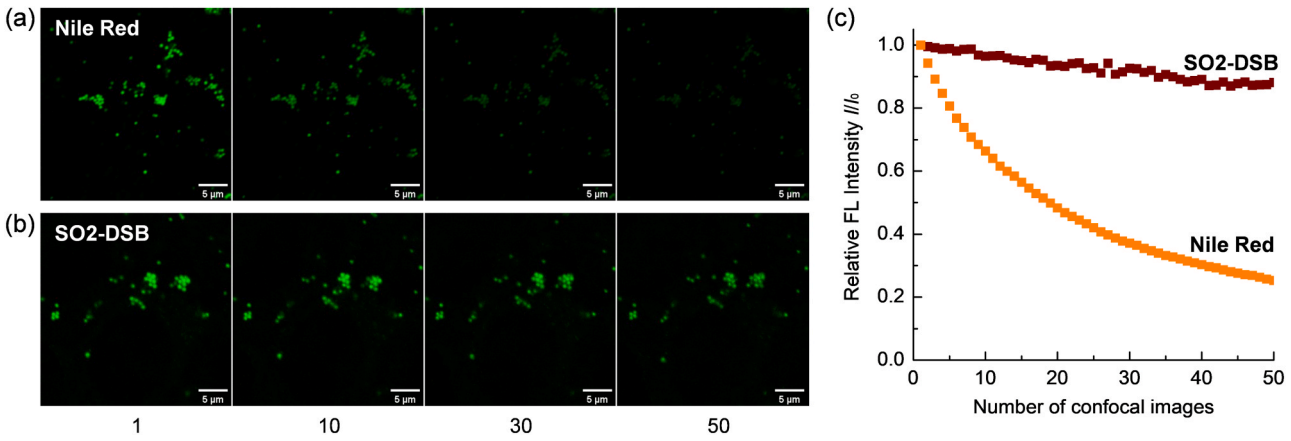

Fig. 3. Comparison of the photostability between Nile Red and SO2-DSB under the confocal imaging with the identical excitation condition (λ_{exc} = 488 nm): (a, b) the confocal images of number 1, 10, 30 and 50, respectively; scale bar: 5 μm; (c) the fluorescence signal intensity of each image (I) relative to the fist image (I_0).

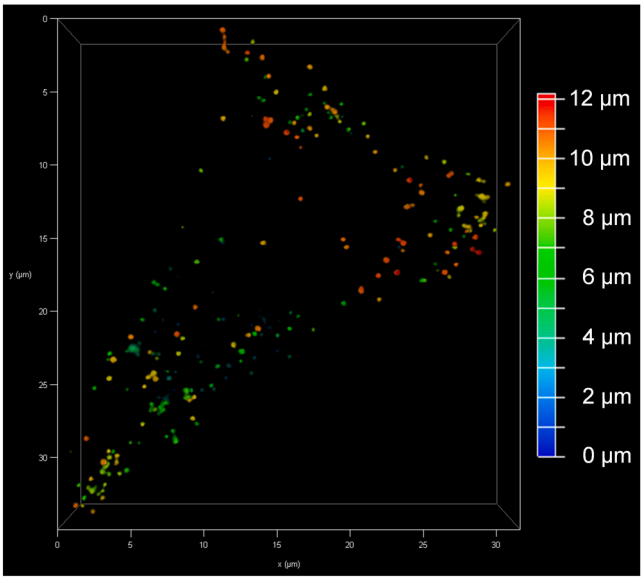

Fig. 4. 3D confocal image of fixed HeLa cells labeled with SO2-DSB. The color variation from blue to red means different Z-depth of lipid droplets.

improve the resolution overcoming the light diffraction limit (~ 250 nm) [16]. Based on this physical process, STED nanoscopy imaging has three prerequisites for the fluorescent probe: 1) the probe should have high photostability to be able to tolerant the extremely strong STED laser; 2) the probe strictly cannot be excited by the STED laser to avoid the donut-shape fluorescence background, *i.e.* the STED laser wavelength should be far away from the absorption spectrum edge of probe (usually more than 50 nm); 3) the fluorescence of probe can be efficiently depleted by the STED laser to get a super-resolution. For the last prerequisite, the probe of which the emission spectrum having large overlap with the STED laser, is usually easy to underdo the depletion process of fluorescence. In consideration of the relationships between the STED laser wavelength and the absorption/emission spectra, the fluorescent probe SO2-DSB featuring with a large Stokes shift should be highly desired for STED nanoscopy imaging.

Initially, the two commonly employed STED lasers (592 nm and 660 nm) were tested to see whether they could be used for the fluorescent probe SO2-DSB. Under the excitation of 592 nm or 660 nm STED laser with a power up to 80 MW cm^{-2}, the HeLa cells stained with probe SO2-DSB did not show any fluorescence signals (Supplementary Fig. S11), excluding the possibility of fluorescence background caused by the extremely strong STED laser. Next, the depletion efficiency of fluorescent probe SO2-DSB was studied. As shown in Fig. 5a, the HeLa cells stained with this probe was imaged under the excitation of 488 nm laser and the depletion of 592 nm STED laser. Keeping the excitation power consistent while gradually increasing the depletion power from 0 to 40 MW cm^{-2}, the fluorescence signal of image had been dramatically depleted. The saturation intensity (I_{sat}) of SO2-DSB, which is defined as the STED laser power required for the half depletion of fluorescent signal and represents one of the key parameters of fluorescent probe for STED nanoscopy imaging, is determined to be 4.0 MW cm^{-2} under the 592 nm STED laser (Fig. 5b). In a similar manner, the I_{sat} of 9.1 MW cm^{-2} is also measured for this fluorescent probe under the 660 nm STED laser (Supplementary Fig. S12). The smaller I_{sat} value under 592 nm STED laser than that of 660 nm STED should be due to that the 592 nm STED laser has larger overlap with the emission spectrum of fluorescent probe. Importantly, the I_{sat} values of SO2-DSB are quite small and even lower than the golden standard STED nanoscopy imaging probe ATTO 647N (10–20 MW cm^{-2}) [24,37] as well as the LDs fluorescent probe Lipi-DSB (10.1 MW cm^{-2}) reported by our group very recently [19]. The low I_{sat} of SO2-DSB means that the stimulated emission depletion process of probe could be easily taken place and the high resolution of fluorescence image can be obtained at low STED power. This is very important for STED nanoscopy imaging because the extremely strong STED laser usually damage the biological samples.

The STED nanoscopy imaging of fluorescent probe SO2-DSB was then comprehensively studied. The living HeLa cells labeled with SO2-DSB was imaged under the 488 nm excitation and the 592 nm depletion. In the confocal image (STED power of 0 MW cm^{-2}), a lot of LDs are very difficult to be distinguished because they are nearby with each other (Fig. 6a and its insets). The full width at half maximum (FWHM) resolution of confocal image is about 228 nm (Fig. 6d). While increasing the STED power to 4 MW cm^{-2} and until to 8 MW cm^{-2}, the STED nanoscopy images provide much more clear LDs (Fig. 6b–c and their insets). The nearby LDs which cannot be separated in the confocal image are finally successfully visualized one by one in the STED images. Accordingly, the FWHM resolutions are largely improved to 148 nm under a STED power of 4 MW cm^{-2} and further reached to 73 nm under a STED power of 8 MW cm^{-2} (Fig. 6e–f). Notably, the resolution of 73 nm is quite fine and represents one of the leading results among the nanoscopy imaging of LDs so far (Supplementary Table S2), particularly in consideration of that this high resolution is obtained under the low STED laser power of 8 MW cm^{-2}.

Besides of 592 nm depletion, another STED laser of 660 nm has also employed for the STED nanoscopy imaging of this fluorescent probe. As shown in Supplementary Fig. S13, the LDs become more and more clear

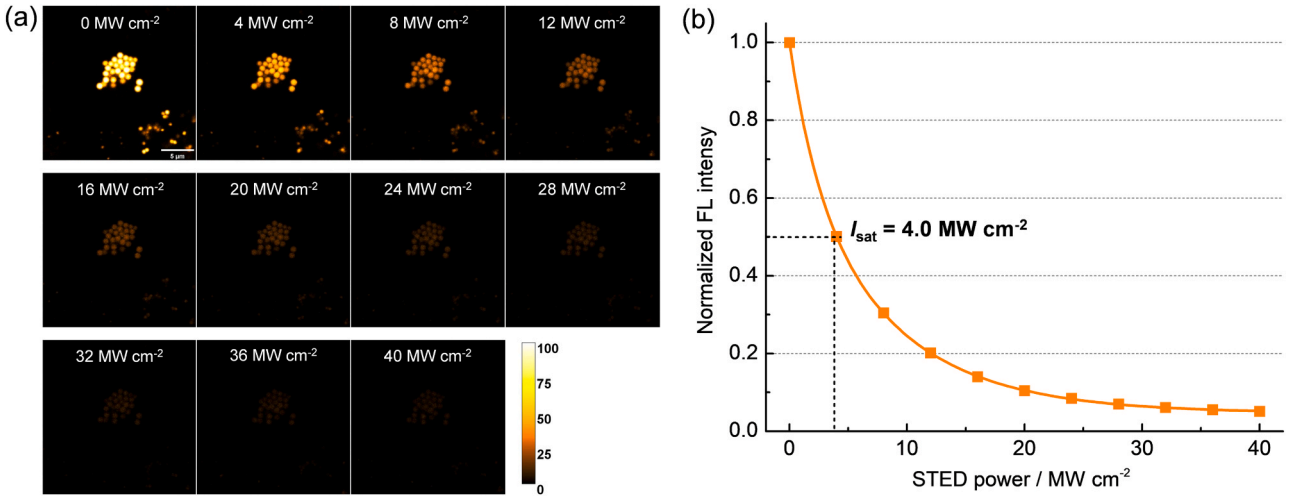

Fig. 5. Stimulated emission depletion efficiency of SO2-DSB: (a) the fluorescence images of HeLa cells labeled with SO2-DSB were recorded under a 488 nm excitation and a 592 nm STED laser (STED laser power of 0–40 MW cm^{-2}); all the images are shown with the same calibration bar of fluorescence brightness; scale bar: 5 μm; (b) the fluorescence signal intensity of each image as a function of the STED laser power.

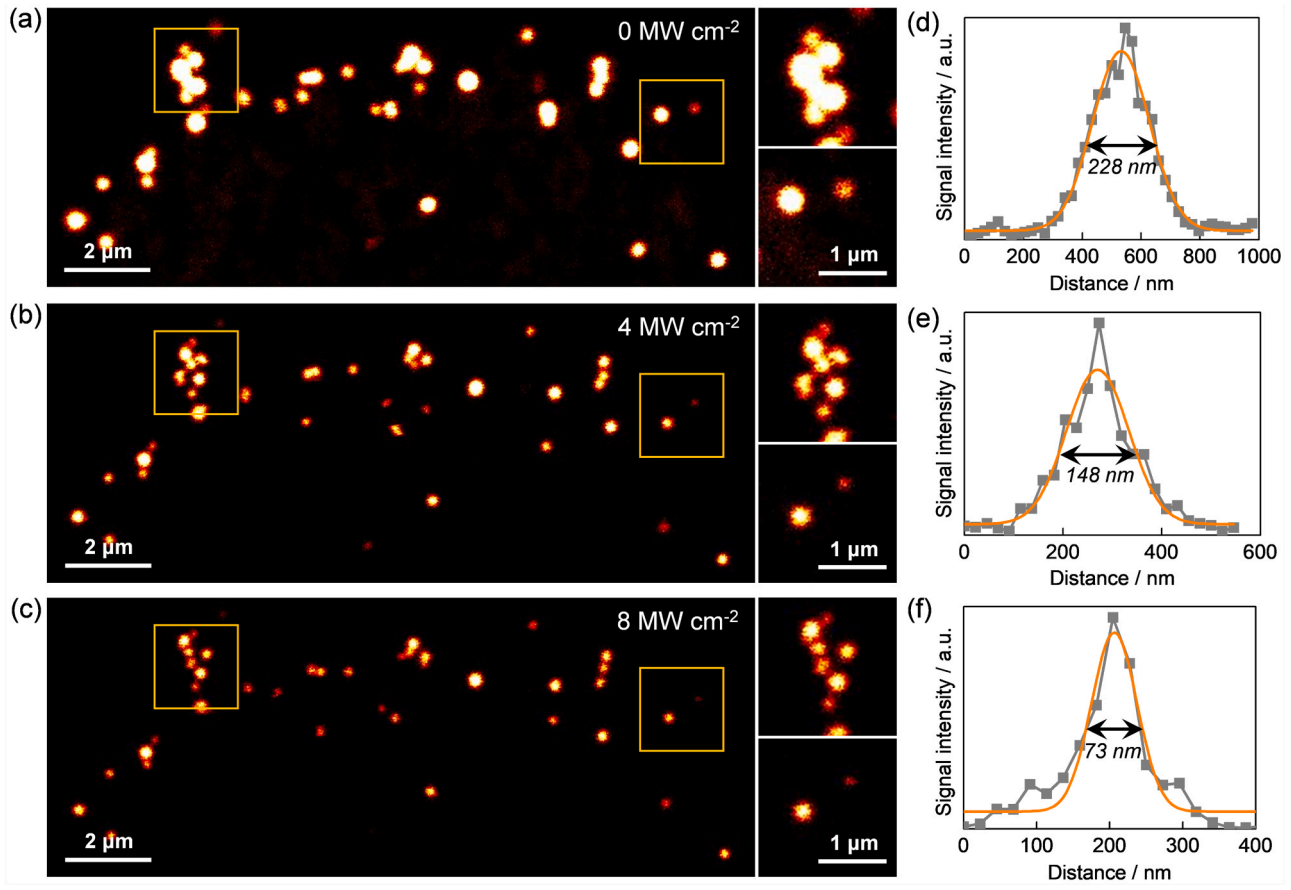

Fig. 6. (a–c) Confocal image and STED nanoscopy images of HeLa cells labeled with SO2-DSB. The images were recorded under excitation at 488 nm and depletion at 592 nm (STED laser powers of 0, 4, and 8 MW cm^{-2}, respectively); scale bar: 2 μm. The insets show zoomed views of the square marked regions; scale bar: 1 μm. (d–f) The FWHM resolutions of confocal and STED images based on the signal intensity profiles (gray lines) crossed the LDs.

upon increasing the 660 nm STED power from 0 to 8 MW cm^{-2}, and until 16 MW cm^{-2}. Accordingly, the FWHM resolutions of images are dramatically improved from 241 nm to 170 nm, and further to 84 nm. The high resolution of 84 nm obtained under the relative low STED power of 16 MW cm^{-2} is outstanding in comparison to the literatures (Supplementary Table S2). The fluorescent probe SO2-DSB, which is capable for the two commonly employed STED lasers (592 nm and 660 nm) and could provide high resolutions under low STED powers, is highly attractive for STED nanoscopy imaging.

3. Conclusion

In summary, we have developed a novel LDs fluorescent probe SO2-DSB featuring with high photostability based on the molecular design strategy of embedding the strong electron-withdrawing sulfone moieties into the distyrylbenzene skeleton. Moreover, this fluorescent probe SO2-DSB displaying large Stokes shift can be easily depleted while be not excited by the commonly used 592 nm or 660 nm STED lasers. These features enable the fluorescent probe to be highly attractive for STED nanoscopy imaging. Consequently, applying this fluorescent probe for STED nanoscopy imaging could precisely visualize the cellular LDs in a nanoscale resolution, which is substantially higher than the common confocal imaging and represents one of the leading results of LDs fluorescence imaging so far. Besides of STED nanoscopy imaging, the 3D confocal imaging and multicolor confocal imaging of this fluorescent probe further increase it values as a powerful tool in the biological study of LDs.

CRediT authorship contribution statement

Guannan Liu: Examined the optical properties, did the cell imaging, wrote the paper. **Jianan Dai:** Synthesized the fluorescent probe. **Ri Zhou:** Analyzed the data. **Guishan Peng**: Analyzed the data. **Chenguang Wang:** Guided the project, wrote the paper. **Xu Yan:** Analyzed the data. **Xiaoteng Jia:** Analyzed the data. **Xiaomin Liu:** Analyzed the data. **Yuan Gao:** Guided the project. **Lijun Wang:** Guided the project. **Geyu Lu:** Guided the project, wrote the paper.

Declaration of Competing Interest

The authors declare that they have no known competing financial interests or personal relationships that could have appeared to influence the work reported in this paper.

Acknowledgements

This work is supported by the National Natural Science Foundation of China (61831011 and 62075079), the China Postdoctoral Science Foundation (2019T120238, 2018M640282, 2020M670847 and 2020T130239), the Natural Science Foundation of Jilin Province (20200201289JC), the Science and Technology Project of Jilin Provincial Department of Education (JJKH20200982KJ).

Appendix A. Supporting information

Supplementary data associated with this article can be found in the online version at doi:10.1016/j.snb.2021.131000.

References

[1] J.A. Olzmann, P. Carvalho, Dynamics and functions of lipid droplets, Nat. Rev. Mol. Cell Biol. 20 (3) (2019) 137–155.
[2] A.R. Thiam, M. Beller, The why, when and how of lipid droplet diversity, J. Cell Sci. 130 (2) (2017) 315–324.
[3] A.R. Thiam, R.V. Farese Jr., T.C. Walther, The biophysics and cell biology of lipid droplets, Nat. Rev. Mol. Cell Biol. 14 (12) (2013) 775–786.
[4] T.C. Walther, R.V. Farese Jr., Lipid droplets and cellular lipid metabolism, Annu. Rev. Biochem. 81 (2012) 687–714.
[5] T.K. Fam, A.S. Klymchenko, M. Collot, Recent advances in fluorescent probes for lipid droplets, Materials 11 (9) (2018) 1768.
[6] M. Collot, T.K. Fam, P. Ashokkumar, O. Faklaris, T. Galli, L. Danglot, A. S. Klymchenko, Ultrabright and fluorogenic probes for multicolor imaging and tracking of lipid droplets in cells and tissues, J. Am. Chem. Soc. 140 (16) (2018) 5401–5411.
[7] L. Guo, M. Tian, Z. Zhang, Q. Lu, Z. Liu, G. Niu, X. Yu, Simultaneous two-color visualization of lipid droplets and endoplasmic reticulum and their interplay by single fluorescent probes in lambda mode, J. Am. Chem. Soc. 143 (8) (2021) 3169–3179.
[8] F. Yu, X. Jing, W. Lin, A unique amphipathic polyethylene glycol-based fluorescent probe for the visualization of lipid droplets and discrimination of living and dead cells in biological systems, Sens. Actuators B: Chem. 302 (2020), 127207.
[9] L. Yang, J. Wang, B. Liu, G. Han, H. Wang, L. Yang, J. Zhao, M. Han, Z. Zhang, Tracking lipid droplet dynamics for the discrimination of cancer cells by a solvatochromic fluorescent probe, Sens. Actuators B: Chem. 333 (2021), 129541.
[10] J. Shi, Y. Tian, B. Guo, Y. Wu, J. Jing, R. Zhang, X. Zhang, An AIEgen-based fluorescent probe for highly selective and specific imaging of lipid droplets in L02 and HepG2 cells, Sens. Actuators B: Chem. 284 (2019) 545–552.
[11] J. Yin, M. Peng, W. Lin, Two-photon fluorescence imaging of lipid drops polarity toward cancer diagnosis in living cells and tissue, Sens. Actuators B: Chem. 288 (2019) 251–258.
[12] M. Jiang, X. Gu, J.W.Y. Lam, Y. Zhang, R.T.K. Kwok, K.S. Wong, B.Z. Tang, Two-photon AIE bio-probe with large Stokes shift for specific imaging of lipid droplets, Chem. Sci. 8 (8) (2017) 5440–5446.
[13] R. Zhou, Y. Cui, J. Dai, C. Wang, X. Liang, X. Yan, F. Liu, X. Liu, P. Sun, H. Zhang, Y. Wang, G. Lu, A. Red-Emissive, Fluorescent probe with a compact single-benzene-based skeleton for cell imaging of lipid droplets, Adv. Opt. Mater. 8 (13) (2020), 1902123.
[14] S.J. Sahl, S.W. Hell, S. Jakobs, Fluorescence nanoscopy in cell biology, Nat. Rev. Mol. Cell Biol. 18 (11) (2017) 685–701.
[15] Y.M. Sigal, R. Zhou, X. Zhuang, Visualizing and discovering cellular structures with super-resolution microscopy, Science 361 (6405) (2018) 880–887.
[16] G. Vicidomini, P. Bianchini, A. Diaspro, STED super-resolved microscopy, Nat. Methods 15 (3) (2018) 173–182.
[17] L. Wang, M.S. Frei, A. Salim, K. Johnsson, Small-molecule fluorescent probes for live-cell super-resolution microscopy, J. Am. Chem. Soc. 141 (7) (2019) 2770–2781.
[18] Z. Liu, J. Liu, X. Wang, F. Mi, D. Wang, C. Wu, Fluorescent bioconjugates for super-resolution optical nanoscopy, Bioconjugate Chem. 31 (8) (2020) 1857–1872.
[19] R. Zhou, C. Wang, X. Liang, F. Liu, X. Yan, X. Liu, P. Sun, H. Zhang, Y. Wang, G. Lu, Stimulated emission depletion (STED) super-resolution imaging with an advanced organic fluorescent probe: visualizing the cellular lipid droplets at the unprecedented nanoscale resolution, ACS Mater. Lett. 3 (5) (2021) 516–524.
[20] M. Taki, K. Kajiwara, E. Yamaguchi, Y. Sato, S. Yamaguchi, Fused thiophene-S,S-dioxide-based super-photostable fluorescent marker for lipid droplets, ACS Mater. Lett. 3 (1) (2021) 42–49.
[21] X. Liu, L. Xin, Z. Tong, W. Du, Z. Yang, H. Cao, S. Wang, Y. Tian, Z. Zhang, R. Zhang, S.C. De Souza, X. Tian, Revealing lipid droplets evolution at nanoscale under proteohormone stimulation by a BODIPY-hexylcarbazole derivative, Biosens. Bioelectron. 175 (2021), 112871.
[22] Y. Xu, H. Zhang, N. Zhang, R. Xu, Z. Wang, Y. Zhou, Q. Shen, D. Dang, L. Meng, B. Z. Tang, An easily synthesized AIE luminogen for lipid droplet-specific super-resolution imaging and two-photon imaging, Mater. Chem. Front. 5 (4) (2021) 1872–1883.
[23] H. Xu, H. Zhang, G. Liu, L. Kong, X. Zhu, X. Tian, Z. Zhang, R. Zhang, Z. Wu, Y. Tian, H. Zhou, Coumarin-based fluorescent probes for super-resolution and dynamic tracking of lipid droplets, Anal. Chem. 91 (1) (2019) 977–982.
[24] X. Yang, Z. Yang, Z. Wu, Y. He, C. Shan, P. Chai, C. Ma, M. Tian, J. Teng, D. Jin, W. Yan, P. Das, J. Qu, P. Xi, Mitochondrial dynamics quantitatively revealed by STED nanoscopy with an enhanced squaraine variant probe, Nat. Commun. 11 (1) (2020) 3699.
[25] C. Wang, M. Taki, Y. Sato, Y. Tamura, H. Yaginuma, Y. Okada, S. Yamaguchi, A photostable fluorescent marker for the superresolution live imaging of the dynamic structure of the mitochondrial cristae, Proc. Natl. Acad. Sci. USA 116 (32) (2019) 15817–15822.
[26] C. Wang, M. Taki, K. Kajiwara, J. Wang, S. Yamaguchi, Phosphole-oxide-based fluorescent probe for super-resolution stimulated emission depletion live imaging of the lysosome membrane, ACS Mater. Lett. 2 (7) (2020) 705–711.
[27] C. Wang, M. Taki, Y. Sato, A. Fukazawa, T. Higashiyama, S. Yamaguchi, Super-photostable phosphole-based dye for multiple-acquisition stimulated emission depletion imaging, J. Am. Chem. Soc. 139 (30) (2017) 10374–10381.
[28] X. Fang, X. Chen, R. Li, Z. Liu, H. Chen, Z. Sun, B. Ju, Y. Liu, S.X.-A. Zhang, D. Ding, Y. Sun, C. Wu, Multicolor photo-crosslinkable AIEgens toward compact nanodots for subcellular imaging and STED Nanoscopy, Small 13 (41) (2017), 1702128.
[29] F. Bottanelli, E.B. Kromann, E.S. Allgeyer, R.S. Erdmann, S.W. Baguley, G. Sirinakis, A. Schepartz, D. Baddeley, D.K. Toomre, J.E. Rothman, J. Bewersdorf, Two-colour live-cell nanoscale imaging of intracellular targets, Nat. Commun. 7 (2016) 10778.
[30] D. Li, W. Qin, B. Xu, J. Qian, B.Z. Tang, AIE nanoparticles with high stimulated emission depletion efficiency and photobleaching resistance for long-term super-resolution bioimaging, Adv. Mater. 29 (43) (2017), 1703643.
[31] C. Spahn, F. Hurter, M. Glaesmann, C. Karathanasis, M. Lampe, M. Heilemann, Protein-specific, multicolor and 3D STED imaging in cells with DNA-labeled antibodies, Angew. Chem. Int. Ed. 58 (52) (2019) 18835–18838.
[32] Z. Man, H. Cui, Z. Lv, Z. Xu, Z. Wu, Y. Wu, Q. Liao, M. Liu, P. Xi, L. Zheng, H. Fu, Organic nanoparticles-assisted low-power STED nanoscopy, Nano Lett. 21 (8) (2021) 3487–3494.
[33] N.I. Shank, H.H. Pham, A.S. Waggoner, B.A. Armitage, Twisted cyanines: a non-planar fluorogenic dye with superior photostability and its use in a protein-based fluoromodule, J. Am. Chem. Soc. 135 (1) (2013) 242–251.
[34] N.I. Shank, K.J. Zanotti, F. Lanni, P.B. Berget, B.A. Armitage, Enhanced photostability of genetically encodable fluoromodules based on fluorogenic cyanine dyes and a promiscuous protein partner, J. Am. Chem. Soc. 131 (36) (2009) 12960–12969.

[35] Y. Oyama, M. Mamada, A. Shukla, E.G. Moore, S.C. Lo, E.B. Namdas, C. Adachi, Design strategy for robust organic semiconductor laser dyes, ACS Mater. Lett. 2 (2) (2020) 161–167.
[36] M.S. Michie, R. Götz, C. Franke, M. Bowler, N. Kumari, V. Magidson, M. Levitus, J. Loncarek, M. Sauer, M.J. Schnermann, Cyanine conformational restraint in the far-red range, J. Am. Chem. Soc. 139 (36) (2017) 12406–12409.
[37] Y. Liu, Y. Ding, E. Alonas, W. Zhao, P.J. Santangelo, D. Jin, J.A. Piper, J. Teng, Q. Ren, P. Xi, Achieving lambda/10 resolution CW STED nanoscopy with a Ti: Sapphire oscillator, PLoS One 7 (6) (2012), e40003.

Guannan Liu received his B.E. degree from Jilin University of China in 2015. He is currently working toward the Ph.D. degree in the Electronics Science and Engineering department, Jilin University. His current researches focus on the organic fluorescent molecules for bio-imaging.

Jianan Dai received his M.S. degree from Jilin University of China in 2019. He is currently working toward the Ph.D. degree in the Electronics Science and Engineering department, Jilin University. His current researches focus on the synthesis of small molecule fluorescent probe and their applications.

Ri Zhou received his M.S. degree from Jilin University of China in 2018. He is currently working toward the Ph.D. degree in the Electronics Science and Engineering department, Jilin University. His current researches focus on the synthesis of small molecule fluorescent probe and their applications.

Guishan Peng received his B.S. degree from Qingdao University of China in 2020. He is currently working toward the M.S. degree in the Electronics Science and Engineering department, Jilin University. His current researches focus on the organic fluorescent molecules for bio-imaging.

Chenguang Wang received his Ph.D. degree from the College of Chemistry, Jilin University in 2013. He then joined the Institute of Transformative Bio-Molecules, Nagoya University as a postdoctoral fellow. In 2019, he joined the College of Electronic Science and Engineering, Jilin University as a professor. His research interests focus on the design and synthesis of organic fluorescent molecules and their applications in fluorescence bio-imaging.

Xu Yan received his Ph.D. degree from the College of Chemistry, Jilin University in 2017. He then joined Prof. Geyu Lu's Group as postdoctoral fellow. In 2019, he joined the College of Electronic Science and Engineering, Jilin University as an associate professor. His research interests mainly focus on the development of functional nanomaterials for chem/bio sensors.

Xiaoteng Jia received her Ph.D. degree from University of Wollongong in 2017. After spend two years as a postdoctoral fellow in Macquarie University and University of California (Irvine), he then joined the College of Electronic Science and Engineering, Jilin University as an associate professor in 2019. His research interests focus on the preparation and application of flexible pressure-sensors.

Xiaomin Liu received her Ph.D. degree from the College of Chemistry, Jilin University in 2008. After spend ten years as an assistant, an associate, and a full professor in Changchun Institute of Optics, Fine Mechanics and Physics, she then moved to the College of Electronic Science and Engineering, Jilin University as professor in 2018. Her research interests focus on the infrared up-conversion photosensitive nanocrystal and a new method for tumor diagnosis and treatment.

Yuan Gao received her Ph.D. degree from Department of Analytical Chemistry at Jilin University in 2012. Now she is an associate professor in Jilin University, China. Her current research is focus on the preparation and application of graphene and semiconductor oxide, especial in gas sensor and biosensor.

Lijun Wang received the B.Sci. degree in electronic sciences in 1973 from Jilin University in China. Now he is a professor of Changchun Institute of Optics, Fine Mechanics and Physics, Chinese Academy of Sciences. His current research interests in basic and applied research of laser technology and other fields.

Geyu Lu received the B.Sci. degree in electronic sciences in 1985 and the M.Sci. degree in 1988 from Jilin University in China and the Dr. Eng. degree in 1998 from Kyushu University in Japan. Now he is a professor of Jilin University, China. His current research interests include the development of chemical sensors and the application of the function materials.